

**TITANIUM DIOXIDE FORMATION VIA  
ANODIZATION AND THERMAL OXIDATION  
FOR PHOTOREDUCTION OF CHROMIUM (VI)**

**NURLIYANA BINTI ABU HASAN SAZALLI**

**UNIVERSITI SAINS MALAYSIA**

**2019**

**TITANIUM DIOXIDE FORMATION VIA  
ANODIZATION AND THERMAL OXIDATION  
FOR PHOTOREDUCTION OF CHROMIUM (VI)**

by

**NURLIYANA BINTI ABU HASAN SAZALLI**

**Thesis submitted in fulfilment of the requirements  
for the degree of  
Master of Science**

**July 2019**

## ACKNOWLEDGEMENT

I would like to express my gratitude to Allah SWT for giving me opportunity to study in Universiti Sains Malaysia (USM) and for enabling me to complete my MSc study there. I would like to extend my sincere gratitude to my supervisor, Assoc. Prof. Dr. Zainovia Lockman. Thank you for your knowledge sharings, patience, support and time throughout my experimental and thesis writing process. I also would like to express my heartfelt thanks to my supervisor`s research team (Nurhaswani Alias, Siti Azlina, Subagja and FYP students). Thank you for the patience, advices, tremendous positive feedbacks given along with the continuous support received.

Not to be forgotten to all the administration and technical staff especially Mr Azzam Rejab, Mr. Kemuridan Md Desa, Mr. Abdul Rasyid Selamat, Madam Haslina Zulkifli, Mr. Azrul Zainol Abidin, Mr. Khairi Khalid, Mr. Zaini, Mr. Syahrul and Mr. Syafiq for their time, assistance and advices. Thank you so much.

Special thanks to both of my parents (Mr. Abu Hasan Sazalli and Madam Zahrah Ahmad) for their endless love and support throughout my studies life. I am truly indebted to them. I also want to give a big thanks to all my siblings, brothers-in-law, sisters-in-law, nieces and nephews for their advices, support and love.

I also would like to say thank you to all mixed mode and full research masters student for the companionship, kindness and support during my study in USM.

Thank you

Nurliyana Abu Hasan Sazalli

9<sup>th</sup> August 2019

## TABLE OF CONTENTS

<b>ACKNOWLEDGEMENT</b> .....	<b>ii</b>
<b>TABLE OF CONTENTS</b> .....	<b>iii</b>
<b>LIST OF TABLES</b> .....	<b>vii</b>
<b>LIST OF FIGURES</b> .....	<b>ix</b>
<b>LIST OF SYMBOLS</b> .....	<b>xiv</b>
<b>LIST OF ABBREVIATIONS</b> .....	<b>xvi</b>
<b>ABSTRAK</b> .....	<b>xviii</b>
<b>ABSTRACT</b> .....	<b>xx</b>
<b>CHAPTER 1 INTRODUCTION</b> .....	<b>1</b>
1.1 Background .....	1
1.1.1 Chromium.....	3
1.1.2 Reduction of Cr(VI) to Cr(III) by photocatalysis process .....	4
1.1.3 Photocatalyst materials for reduction of Cr(VI).....	5
1.1.4 Anodic and thermal oxidation for TiO <sub>2</sub> Nanotubes and Nanowires Formation.....	7
1.2 Problem Statement .....	8
1.3 Research Objectives .....	10
1.4 Research Scope .....	10
1.5 Thesis Outline .....	11
<b>CHAPTER 2 LITERATURE REVIEW</b> .....	<b>12</b>
2.1 Introduction .....	12
2.2 Titanium .....	12
2.3 Titanium dioxide .....	14
2.3.1 Rutile .....	17
2.3.2 Anatase .....	18

2.3.3	Semiconductor materials .....	18
2.4	Nanostructure of TiO <sub>2</sub> .....	18
2.4.1	Nanomaterials .....	18
2.4.2	Nanostructure of TiO <sub>2</sub> .....	19
2.5	Synthesis of titanium dioxide .....	20
2.5.1	Electrochemical anodic oxidation method .....	21
2.5.1(a)	Mechanism of compact and dense TiO <sub>2</sub> formation .....	22
2.5.1(b)	Mechanism of nanotubes TiO <sub>2</sub> formation .....	23
2.5.1(c)	Effect of fluoride presence in anodization electrolyte .....	28
2.5.1(d)	Effect of voltage .....	31
2.5.2	Thermal oxidation method.....	34
2.5.2(a)	Mechanism.....	35
2.5.2(b)	Effect of KOH catalyst presence .....	36
2.5.2(c)	Effect of temperature .....	38
2.6	Photocatalysis reduction of Cr(VI).....	40
2.6.1	TiO <sub>2</sub> photocatalytic activity for Cr removal .....	42
<b>CHAPTER 3 METHODOLOGY .....</b>		<b>44</b>
3.1	Introduction .....	44
3.2	Raw materials and chemicals .....	44
3.3	Stage 1: Synthesis of materials.....	46
3.3.1	Anodic oxidation .....	46
3.3.1(a)	Foil preparation.....	46
3.3.1(b)	Electrolyte preparation .....	48
3.3.1(c)	Anodization .....	48
3.3.1(d)	Cleaning of NTs and thermal annealing .....	48
3.3.2	Thermal oxidation for TiO <sub>2</sub> nanowires formation.....	49
3.3.2(a)	Foil preparation.....	49

3.4	Stage 2: Characterization techniques .....	50
3.4.1	Field Emission Scanning Electron Microscope (FESEM) .....	50
3.4.2	Transmission Electron Microscope (TEM) .....	51
3.4.3	Energy Dispersive X-ray (EDX) Spectroscopy .....	52
3.4.4	X-ray Diffraction (XRD) .....	53
3.4.5	RAMAN Spectroscopy .....	54
3.4.6	Fourier Transform Infrared (FTIR) Spectroscopy .....	56
3.4.7	Ultraviolet-visible (UV-VIS) Spectroscopy .....	57
3.5	Stage 3: Photocatalytic Experiment .....	57
3.5.1	Preparation of Chromium Stock Solution .....	57
3.5.2	Photocatalysis Experiment .....	58
3.5.3	Cr(VI) Reduction Analysis .....	59
<b>CHAPTER 4 RESULTS AND DISCUSSION .....</b>		<b>60</b>
4.1	Introduction .....	60
4.2	Anodic oxidation of TiO <sub>2</sub> .....	60
4.2.1	Anodization for Compact TiO <sub>2</sub> Formation .....	60
4.2.1(a)	Morphological Analysis .....	60
4.2.1(b)	Structural Analysis .....	63
4.2.2	Effect of Voltage .....	64
4.2.2(a)	Morphological Analysis .....	64
4.2.2(b)	Structural Analysis .....	73
4.2.3	Photocatalytic Experiment .....	77
4.2.3(a)	Photocatalytic reduction of Cr(VI) for anodic oxidized samples under UV light .....	77
4.3	Thermal oxidation of titanium .....	80
4.3.1	Oxidation for compact and dense TiO <sub>2</sub> formation .....	80
4.3.1(a)	Morphological Analysis .....	81
4.3.1(b)	Structural Analysis .....	82

4.3.1(c)	Mechanism.....	83
4.3.2	Effect of Temperature.....	84
4.3.2(a)	Morphological Analysis .....	84
4.3.2(b)	Structural Analysis .....	87
4.3.2(c)	Mechanism.....	89
4.3.3	Photocatalysis reduction experiment .....	90
4.3.3(a)	Photocatalytic reduction of Cr(VI) for thermal oxidized samples under UV light .....	90
4.3.3(b)	Photocatalytic reduction of Cr(VI) mechanism by thermal oxidized samples under UV light.....	93
<b>CHAPTER 5 CONCLUSION AND RECOMMENDATIONS.....</b>		<b>98</b>
5.1	Conclusion.....	98
5.2	Recommendations .....	98
<b>REFERENCES.....</b>		<b>100</b>

## LIST OF TABLES

	<b>Page</b>
Table 2.1 Characteristics of Ti when compared to other metals (Lütjering and Williams, 2007).....	13
Table 2.2 Different phases of TiO <sub>2</sub> (Hanaor and Sorrell, 2011). ....	15
Table 2.3 Bulk properties of titanium dioxide with its crystal structures (Diebold, 2003). ....	16
Table 2.4 Summary on the early study of anodic titanium film.....	28
Table 2.5 Effect of anodization voltages on anodised Ti. ....	33
Table 2.6 Comparison between various method for Cr(VI) removal. ....	40
Table 2.7 Summary of published research study on TiO <sub>2</sub> NTs and NWs for Cr(VI) reduction.....	43
Table 3.1 Raw materials and chemicals that were used in this project.....	45
Table 3.2 Summary of parameters used for compact and TiO <sub>2</sub> NTs formation. ....	48
Table 3.3 Oxidation conditions for the formation of compact and NWs structure....	50
Table 4.1 EDX of the as-anodized sample (anodization was done in EG/H <sub>2</sub> O at 60 V for 30 min).....	62
Table 4.2 EDX of the annealed sample (annealing was done at 400°C in air environment for 3 h).....	62
Table 4.3 Dimensions of annealed TNTs samples prepared at 20 V, 40 V and 60 V (annealing was done at 400°C in air environment for 3 h). ....	70
Table 4.4 EDX result of as-anodized TNTs (anodization was done in EG/NH <sub>4</sub> F/H <sub>2</sub> O at 20 V, 40 V and 60 for 30 min). ....	72
Table 4.5 EDX result of annealed TNTs samples prepared at 20 V, 40 V and 60 V (annealing was done at 400°C in air environment for 3 h). ....	72
Table 4.6 EDX result of thin and compact oxidised Ti foil at 700°C for 2 hours in air environment. ....	82



Table 4.7 Diameter and length of oxidised Ti foil at 700°C, 650°C, 600°C and 550°C.....	86
Table 4.8 EDX analysis on oxidised Ti foils with KOH catalyst at 550 - 700°C for 2 hours.....	86
Table 4.9 Phases of all four systems of photocatalyst in this work .....	96
Table 4.10 Comparison of this project with previous reported work .....	97

## LIST OF FIGURES

	<b>Page</b>
Figure 1.1 Photo-activation of a semiconductor and primary reactions occurring on its surface (Colmenares and Luque, 2014).....	5
Figure 2.1 Crystal structure of HCP and BCC phase (Layens and Peters, 2003).....	14
Figure 2.2 Planar $Ti_3O$ building-block representation (left) and $Ti_6O$ polyhedral (right) for the $TiO_2$ phases rutile (a), anatase (b) and brookite (c) (Ti (white); O (red)) (Landmann et al., 2012).....	16
Figure 2.3 Comparison of electron pathways through $TiO_2$ nanoparticles (NPs), nanotubes (NTs) and nanorods (NRs). (a-b) (Javed et al., 2014) (c) (Sengupta et al., 2016) .....	20
Figure 2.4 Schematic drawing for Titanium anodization cell (Galstyan et al., 2013). .....	22
Figure 2.5 Schematic drawing for anodization of titanium in an electrolyte free from fluoride ions (Macak et al., 2007) .....	23
Figure 2.6 Current-time anodizing curve (Kowalski et al., 2013) .....	25
Figure 2.7 Schematic of the electrochemical anodization (a) experiment setup, (b) mechanism of $TiO_2$ NTs deposition (Awad et al., 2017).....	26
Figure 2.8 Schematic representation on the transformation from a porous to tubular nanostructure (Khudhair et al., 2016).....	26
Figure 2.9 Schematic drawing for anodization of titanium in an electrolyte with presence of fluoride ions (Khudhair et al., 2016).....	28
Figure 2.10 Anodised Ti surface (a) Blisters and microcracks, (b) Grain boundary area (Sibert, 1963).....	30
Figure 2.11 Film thickness, Å as a function of forming voltage, V (Sibert, 1963) ...	30
Figure 2.12 Surface view of an-anodised $TiO_2$ (Aladjem et al., 1970) .....	31
Figure 2.13 FESEM images of $TiO_2$ NTs array surface anodised at 50 V, 52 V, 55 V and 57 V. ....	32

Figure 2.14 Diagram of silicon growth by VLS mechanism. (a) Initial condition with Au-Si liquid droplet (b) Nanowire growth with Au-Si liquid droplet on top of the wire (Wagner and Ellis, 1964).....	35
Figure 2.15 SEM images of oxidised titanium foil at 650°C for 2 hours in water vapour; a) with KF, b) without KF (Cheung et al., 2007); SEM images of oxidized thin film of titanium at 650°C for 4 hours in hydrogen and argon c) with KOH, d) without KOH (Lee, 2014).....	37
Figure 2.16 SEM images of oxidised pure titanium foil at temperature (a) 650°C, (b) 700°C, (c) 750°C, (d) 800°C and (e) 850°C in acetone environment for 1.5 h.....	39
Figure 2.17 Effect of temperature on titanium oxidation with the presence of a catalyst at a) 450°C b) 550°C and c) 650°C (Cheung et al., 2007) ....	39
Figure 3.1 Flowchart for procedures of experiment.....	47
Figure 3.2 Annealing profile for annealing process of TiO <sub>2</sub> NTs.....	49
Figure 3.3 Heating profile for formation of TiO <sub>2</sub> NWs. ....	50
Figure 3.4 Photographs of Raman spectrophotometer.....	56
Figure 3.5 Experimental set-up for photoreduction test of Cr(VI) in custom-made UV reactor.....	58
Figure 4.1 Photographs of (a) as-anodized titanium in EG/H <sub>2</sub> O electrolyte at 60 V for 30 min and (b) as-annealed anodised titanium (60 V, 30 min) at 400 °C for 3 h in air .....	61
Figure 4.2 Current densities-time plot of Ti foil during anodization in EG/H <sub>2</sub> O electrolyte at 60 V. ....	61
Figure 4.3 Surface FESEM images of annealed TiO <sub>2</sub> compact in air environment for 3 hour at 400°C.....	62
Figure 4.4 XRD result of compact as-anodized (ANO) and annealed (ANN) TiO <sub>2</sub> samples.....	63
Figure 4.5 Raman analysis of thin and compact layer of as-anodized (ANO) under 60 V for 30 min and annealed (ANN) Ti samples at 400°C under air environment for 3 hours.....	64

Figure 4.6 Physical appearance of Ti foil (top) as-anodized (ANO) in EG/NH <sub>4</sub> F/H <sub>2</sub> O electrolyte for 30 min and (bottom) annealed (ANN) at 400°C for 3 h in air environment. ....	65
Figure 4.7 Current density, J against time, t of Ti foil during anodization in EG/NH <sub>4</sub> F/H <sub>2</sub> O electrolyte at 20 V, 40 V and 60 V. ....	66
Figure 4.8 FESEM images of TiO <sub>2</sub> NTs (oxide surface and cross section) (a-b) as-anodized Ti in EG/NH <sub>4</sub> F/H <sub>2</sub> O electrolyte for 30 min at 20 V and (c-d) annealed Ti in air environment for 3 hour at 400°C.....	68
Figure 4.9 FESEM images of TiO <sub>2</sub> NTs (oxide surface and cross section) (a-b) as-anodized Ti in EG/NH <sub>4</sub> F/H <sub>2</sub> O electrolyte for 30 min at 40 V and (c-d) annealed Ti in air environment for 3 hour at 400°C.....	68
Figure 4.10 FESEM images of TiO <sub>2</sub> NTs (oxide surface and cross section) (a-b) as-anodized Ti in EG/NH <sub>4</sub> F/H <sub>2</sub> O electrolyte for 30 min at 60 V and (c-d) annealed Ti in air environment for 3 hour at 400 °C.....	69
Figure 4.11 FESEM images of TiO <sub>2</sub> NTs (oxide surface and cross section) as-anodized Ti in EG/NH <sub>4</sub> F/H <sub>2</sub> O electrolyte for 30 min at 80 V. ....	69
Figure 4.12 TEM images of annealed TNTs samples prepared at 60 V (annealing was done at 400°C in air environment for 3 h). ....	71
Figure 4.13 XRD patterns for the as-anodized TNTs (anodization was done in EG/NH <sub>4</sub> F/H <sub>2</sub> O at 20 V, 40 V and 60 for 30 min). ....	73
Figure 4.14 XRD patterns of annealed TNTs samples prepared at 20 V, 40 V and 60 V (annealing was done at 400°C in air environment for 3 h). ....	74
Figure 4.15 Raman spectra of as-anodized TNTs (anodization was done in EG/NH <sub>4</sub> F/H <sub>2</sub> O at 20 V, 40 V and 60 for 30 min) and annealed TNTs 20, 40 and 60 V samples (annealing was done at 400°C in air environment for 3 h). ....	75
Figure 4.16 FTIR spectra of as-anodized TNTs (anodization was done in EG/NH <sub>4</sub> F/H <sub>2</sub> O at 20 V, 40 V and 60 for 30 min). ....	76
Figure 4.17 FTIR result of annealed TNTs (annealing was done at 400°C in air environment for 3 h).....	76

Figure 4.18 Photoreduction of Cr(VI) solution at different pH on annealed TNTs prepared at 40 V (annealing was done at 400°C in air environment for 3 h).....	77
Figure 4.19 Schematic diagram of Cr(VI) solution colour changes before and after added with one drop of DPC.....	78
Figure 4.20 Comparison of photoreduction of Cr(VI) result between compact anodic oxidised and NTs TiO <sub>2</sub> (60V) samples irradiated with UV light for 60 min. ....	79
Figure 4.21 Comparison of photoreduction of Cr(VI) result between NTs TiO <sub>2</sub> samples anodised at different potential irradiated with UV light for 60 min. ....	80
Figure 4.22 Photographs of Ti foils; (a) as-received, (b) XXXX, and (c) oxidised at 700 °C in air. ....	81
Figure 4.23 FESEM images of compact oxidised Ti foil at 700°C for 2 hours in air environment. The inset shows FESEM image of oxide surface at higher magnification level.....	81
Figure 4.24 XRD pattern for the compact TiO <sub>2</sub> film after thermal oxidation of titanium at 700°C in air. ....	82
Figure 4.25 Raman shift of compact TiO <sub>2</sub> film formed at 700°C for 120 min in air. ....	83
Figure 4.26 Photographs of Ti foil before and after oxidised at 500 - 750°C in KOH environment for 120 min.....	84
Figure 4.27 FESEM images of oxidised Ti foils at (a-b) 700 °C (c-d) 650 °C (e-f) 600 °C (g-h) 550 °C and (i-j) 500 °C with KOH deposition in air.....	85
Figure 4.28 TEM images of TiO <sub>2</sub> NWs thermally oxidised at 700°C for 120 min. ..	87
Figure 4.29 XRD pattern of oxidised Ti foils with KOH catalyst at 500 - 700°C for 2 hours. ....	88
Figure 4.30 Raman shift for oxidised Ti foils in the presence of KOH at 550 – 700°C for 120 min. `R` in the figure indicates rutile phase. ....	89

Figure 4.31 Comparison of photoreduction of Cr(VI) result between compact thermal oxidised and NWs TiO <sub>2</sub> (700°C) samples irradiated with UV light for 60 min.....	92
Figure 4.32 Comparison of photoreduction of Cr(VI) result between NWs TiO <sub>2</sub> samples oxidised at 550-700°C irradiated with UV light for 60 min. ....	92
Figure 4.33 Summary of four systems of photocatalyst in this work .....	95

## LIST OF SYMBOLS

$\text{g/cm}^3$	Gram per centimeter cube
%	Percentage
<	Less than
>	More than
°	Degree
°C	Degree celcius
°C/min	Degree celcius per minute
$\theta$	Bragg angle
$\lambda$	Wavelength
$\bullet\text{O}_2^-$	Superoxide radical
$\bullet\text{OOH}$	Hydroperoxyl radical
$\bullet\text{OH}$	Hydroxyls radical
A	Ampere
Å	Angstrom ( $10^{-10}$ m)
cm	Centimeter
$E_g$	Band gap
$\text{cm}^3$	Centimeter cube
$E_{CB}$	Conduction band edge potential
$I$	Current
$i$	Critical current density
D	Diameter
$e^-$	Electron
eV	electronvolt

g	Gram
h	hour
L	Length
mg	Milligram
$\mu\text{m}$	Micrometer
mm	millimeter
mL	Milliliter
M	Molarity
min	Minute
nm	Nanometer
d	Oxide thickness
h $\nu$	Photon energy
%	Percentage
s	Second
T	Temperature
$E_{\text{VB}}$	Valence band edge potential
V	Volt
wt.%	Weight percentage
$2\theta$	Diffraction angle



## LIST OF ABBREVIATIONS

1D	One-dimensional
a.u.	Arbitrary unit
CB	Conduction band
Cr(III)	Trivalent chromium
Cr(VI)	Hexavalent chromium
DI	Deionized
DOE	Department of Environment
EDTA	Ethylenediaminetetraacetic acid
EDX	Energy dispersive X-ray
EG	Ethylene glycol
EPA	Environmental Protection Agency
FESEM	Field Emission Scanning Electron Microscope
FRL	Fluoride-rich layer
FTIR	Fourier-transform Infrared
FWHM	Full width height maximum
IARC	International Agency for Research on Cancer
IR	Infrared
ISO	International Organization for Standardization
J-t	Current density-time
NHE	Normal hydrogen electrode
NPs	Nanoparticles
NTs	Nanotubes
NWs	Nanowires

PDF	Powder diffraction file
pH	Hydrogen potential
SC	Semiconductor
TEM	Transmission Electron Microscope
TNTs	Titanium dioxide nanotubes
US-EPA	US Environmental Protection Agency
UV	Ultraviolet
UV-Vis	Ultraviolet-visible
VB	Valence band
vs	Versus
WHO	World Health Organization
XRD	X-ray Diffraction

# **PENGHASILAN TITANIUM DIOKSIDA MELALUI PENGANODAN DAN PENGOKSIDAAN TERMAL UNTUK FOTOMANGKIN KROMIUM (VI)**

## **ABSTRAK**

Kajian ini menyiasat kebolehan fotomangkin untuk menurunkan Cr(VI) kepada Cr(III) di dalam larutan akueus TiO<sub>2</sub> berstruktur nano (tiub nano (TNTs) dan dawai nano (NWs)) melalui pengoksidaan anodik dan termal, masing-masing. TNTs dihasilkan dalam elektrolit yang mengandungi fluorida sementara NWs TiO<sub>2</sub> di hasilkan dalam persekitaran oksida yang mengandungi potassium. Semasa proses penghasilannya, di jumpai TiO<sub>2</sub> mengandungi ion-ion yang kewujudannya diperlukan bagi menghasilkan struktur nano. Bahan cemar utama yang menduduki dalam oksida NTs dan NWs ialah ion fluorida dan potassium, masing-masing. EDX dan SEM telah digunakan untuk mengkaji kuantiti bahan cemar di dalam oksida tersebut. TNTs mengandungi 1.89 wt% fluorin. NWs mengandungi 7.54% potassium. Oleh hal yang demikian, bagi membandingkan sama ada bahan cemar tersebut memberi kesan terhadap proses penurunan Cr(VI), filem TiO<sub>2</sub> telah di hasilkan secara pengoksidaan anodik dan termal tanpa kehadiran ion fluorida dan potassium, masing-masing. Hasilnya ialah filem berstruktur padat tanpa sebarang kehadiran struktur nano. Mengikut EDX, filem-filem itu bebas daripada bahan cemar. Fasa penghabluran bagi oksida TiO<sub>2</sub> anodik dan termal ini juga di kaji. TNTs mengandungi anatase seperti mana di dapati daripada XRD dan spektroskopi Raman sementara anodik TiO<sub>2</sub> padat mengandungi amorfus dan rutil. Kedua-dua oksida termal TiO<sub>2</sub> mengandungi rutil. Filem NTs, NWs dan padat TiO<sub>2</sub> telah di uji di dalam eksperimen fotokatalisis bagi menurunkan Cr(VI) kepada Cr(III). Anodik TiO<sub>2</sub> padat berjaya menurunkan sebanyak 48.36% Cr(VI) selepas 20 minit. Manakala, TNTs yang telah di sepuh lindap dapat menurunkan 5.86% Cr(VI) selepas 20 minit. Ini menunjukkan TNT mempunyai kurang keupayaan menurunkan Cr(VI) berbanding filem padat anodik. Dalam masa yang sama,

TiO<sub>2</sub> padat yang telah di oksida secara termal menurunkan 28.04% Cr(VI) berbanding 14.48% oleh NWs selepas 20 minit. Walaubagaimanapun, selepas 50 minit, kesemua empat struktur TiO<sub>2</sub> telah menghampiri 100% tahap penurunan.

# **TITANIUM DIOXIDE FORMATION VIA ANODIZATION AND THERMAL OXIDATION FOR PHOTOREDUCTION OF CHROMIUM (VI)**

## **ABSTRACT**

This study investigated on the photocatalytic performance to reduce Cr(VI) to Cr(III) in aqueous solution of TiO<sub>2</sub> nanotubes (NTs) and nanowires (NWs) synthesised by oxidation of titanium, anodically and thermally, respectively. TiO<sub>2</sub> NTs were produced in fluoride containing electrolyte whereas TiO<sub>2</sub> NWs were produced in potassium containing oxidation environment. During these fabrication processes, TiO<sub>2</sub> was found to contain ions which were required for the growth of the nanostructures. In NWs, potassium ions were found to be the main impurity whereas in NTs, fluoride ions were detected to be incorporated within the oxide. EDX in SEM was used to study the amount of impurities in the oxide. It was found that anodic TNTs were consisted of 1.89 wt % of fluorine. Thermally oxidised NWs contained 7.54 wt% of potassium contamination. Therefore, as to compare if the impurities affect the Cr(VI) reduction process, TiO<sub>2</sub> films were also created either by anodic or thermal oxidation in the absence of fluoride ions and potassium ions, respectively. The resulting films were compact without any noticeable nanostructures and from EDX the films were free from contamination. The crystal phases of the anodic or thermal oxidised TiO<sub>2</sub> were also studied. It was found that anodic NTs were comprised of anatase as shown from XRD and Raman spectroscopy whereas compact TiO<sub>2</sub> was consisted of a mixture of amorphous and rutile. Thermally oxidised TiO<sub>2</sub> compact and NWs on the other hand were consisted of both rutile oxide. NTs, NWs and compact TiO<sub>2</sub> were tested in a photocatalysis experiment to reduce Cr(VI) to Cr(III). It was found that compact anodised TiO<sub>2</sub> can reduce down to 48.36% after 20 minutes. Whereas annealed NTs

can reduce 5.86% after 20 min. This indicated that the NTs have less ability to reduce Cr(VI) compared to compact anodic film. Similarly, thermally oxidised titanium with compact structure can reduce 28.04% compared to 14.48% NWs after 20 min. However, it was found that after 50 min , all four samples has reach almost 100% of reduction.

# CHAPTER 1

## INTRODUCTION

### 1.1 Background

Industrial growth has many advantages. However, the flow of the unregulated industrial waste especially wastewater into the waterways has resulted in pollution-related diseases to animals, plants and humans. According to Schneider (2014), in the recent two decades, the pollutants, coming from a variety of industrial activities, are contaminating surface and ground water to an unacceptable level all over the world. The discharged water if not properly treated is contaminated with toxic organic and inorganic compounds (Chen et al., 2000) which are harmful to the environment.

Examples of inorganic compounds are heavy metal ions. Heavy metals are elements with an atomic density greater than  $6 \text{ g/cm}^3$ . They are one of the most persistent pollutants in wastewater. Among the various manufacturing sectors that contribute to the high concentrations of heavy metal ions in their wastewater are metal finishing processes including steel polishing, chrome plating and etching. Textile industries also contribute to heavy metal such as cadmium (Cd), lead (Pb), chromium (Cr) and copper (Cu) pollutions as many dyes and pigments washed away in the waste water containing heavy metal ions (Pang and Abdullah, 2013). Indeed, there have been many studies evaluating the distribution of heavy metals such as zinc (Zn) (Mokhtar et al., 2015), nickel (Ni) (Sakai et al., 2017), iron (Fe) (Khodami et al., 2017), arsenic (As) (Looi et al., 2013), mercury (Hg) (Looi et al., 2015), cadmium (Cd) (Khodami et al., 2017) and chromium (Cr) (Praveena and Lin, 2015) in the water near to industrial areas. All of these works reach a consensus that the problem of heavy metal pollution,

despite can be controlled, must be acknowledged as to reduce the amount of such pollutants in the water.

In Malaysia, 51 rivers (11%) are reported to be polluted based on the Department of Environment Malaysia (DOE), Malaysia report in 2017. Among the pollutants reported are As, Fe, Manganese (Mn) and Ni (Affandi and Ishak, 2018). The presence of these metals or metalloids in water can induce perturbation of ecological and geological equilibrium because they have generally infinite lifetimes (Litter, 2015). There is therefore an urgent need to ensure manufacturers and waste generating industries are compliant with the environmental acts as to ensure zero contamination and there should also be better control of pollution from wastewater in the country.

Hexavalent Cr or Cr(VI) is a heavily toxic, mutagenic and carcinogenic metal to most of the living organisms (Suksabye et al., 2009) when its concentration level is higher than 0.05 ppm. Cr(VI) is also corrosive and extremely mobile than Cr(III) (Ku and Jung, 2001). However, Cr(VI) compounds have been widely utilized in various industrial processes especially steel and plating industries for centuries. Cr(VI) has also been used as pigments, dyes (Halimoon and Yin, 2010), chemical manufacture, leather tannery (Chen et al., 2012), metal plating (Cavaco et al., 2007), and fertilizer manufacturer (Bankole et al., 2014). These manufacturers can also be responsible in high level of Cr(VI) pollution in river water. Unless properly treated, Cr(VI) can be easily discharged to the environment.

There have been reports recently on the amount of Cr in Malaysia. For example, Praveena and Lin (2015) reported that the levels of Cr in some of the fish in Port Dickson such as *Selaroides* spp (2.34 mg/kg) and *Sardinella* spp (1.42 mg/kg) had exceeded the limit (1 mg/kg) enforced by the Malaysian Food Regulations (1985). Another researcher also found high concentration of Cr (4.205 mg/kg) in red snapper



fish in Pulau Ketam near Port Klang, Selangor. Apart from red snapper, Cr has also been detected in many other types of fish (Widad and Abdullah, 2013, Poon et al., 2016). Existence of Cr in seafood must be taken as serious issue due to the danger of accumulation in the food chain. Upon consumption, Cr(VI) can retain in human body, in which it accumulates throughout life. Excessive exposure of Cr(VI) can result in acute irritant to human leading to allergen. Not only that, when Cr(VI) is digested for instance by consuming water or seafood contaminated by Cr(VI), it can cause diarrhoea, internal haemorrhage or kidney damage. Hence, assessment on the amount of Cr(VI) released from the industrial establishment as well as method of removal of Cr(VI) from wastewater is very much needed. In this work, a process to remove Cr(VI) from stimulated wastewater is proposed via photocatalytic reduction.

### **1.1.1 Chromium**

Chromium has five oxidation states. Oxidation state of +3 is considered essential for good health in moderate intake, however, chromium in oxidation state of +6 (Cr(VI)) is considered harmful even in small intake quantity (Guertin et al., 2016). Cr(VI) is the second most stable oxidation state of chromium and has been categorised as Group 1 materials which is human carcinogen by International Agency for Research on Cancer (IARC), France by inhalation. On the other hand, consuming excessive amount of Cr(VI) can cause severe health problems such as damage of liver and kidney as well as the central nerve system (Sharma, 2014).

According to World Health Organization (WHO) International Standards for Drinking water, the maximum allowable concentration of Cr(VI) is 0.05 mg/L (Organization, 2011). In the United States, the Environmental Protection Agency

(EPA) under the authority of the Safe Drinking Water Act (SDWA) has set the maximum contaminant level of Cr(VI) at 0.10 mg/L while in Malaysia, parameter limits of effluent of Cr(VI) is 0.005 mg/L based on Environmental Quality Act, 1974 and the Malaysia Environmental Quality (Sewage and Industrial Effluents) Regulations, 1979, 1999, 2000. Chromium (III) is an essential element in humans, with a daily intake of 50 to 200 µg/d recommended for adults. Ensuring water free from Cr(VI) contamination is crucial.

There are many methods that can be used to remove Cr(VI) from wastewater such as biological method, ion exchange (Rengaraj et al., 2003), bioremediation, membrane separation (Modrzejewska and Kaminski, 1999), adsorption (Rao et al., 2002), biosorption (Ziagova et al., 2007), chemical precipitation (Chen et al., 2007), ozonation chemical reduction and photocatalytic reduction (Athanasakou et al., 2017, Chen et al., 2017, Cheng et al., 2015, Li et al., 2017). However, apart from photocatalytic reduction, many of them suffer from limitations such as generating sludge, not fully precipitating, high operational cost and zero removal is almost impossible (Güell et al., 2008, Litter, 2015). Photocatalysts reduction can be adopted for Cr(VI) removal whereby Cr(VI) is reduced to Cr(III) in the presence of photocatalysts under light illumination. Photocatalysis is a one-step removal process, therefore it also has the advantage to be more practical and cleaner than chemical reduction, hence, it is a preferred method to transform Cr(VI) to Cr(III).

### **1.1.2 Reduction of Cr(VI) to Cr(III) by photocatalysis process**

Photocatalysis is a process that uses photons from the UV-near visible region (Barakat, 2011) to illuminate a solid catalyst as to generate free electrons within the material (Kisch and Hennig, 1983, Serpone and Pelizzetti, 1989). A photocatalyst is

often oxide semiconductor. When the semiconductor (SC) is irradiated by photon with energy higher than its band gap energy which is illustrated in Figure 1.1, the electron-hole pairs are formed on the surface of the SC. The excitation process occurs when electrons in the valence band of the SC absorbed the photon energy and make a transition to the conduction band leaving behind holes. Photogenerated electrons can be used for reduction processes whereas photogenerated holes can be used for oxidation to happen. As for Cr(VI) reduction, holes can lead to the transformation of H<sub>2</sub>O to oxygen and Cr(VI) to Cr(III) reduction can be done by the electrons (Litter, 2015).

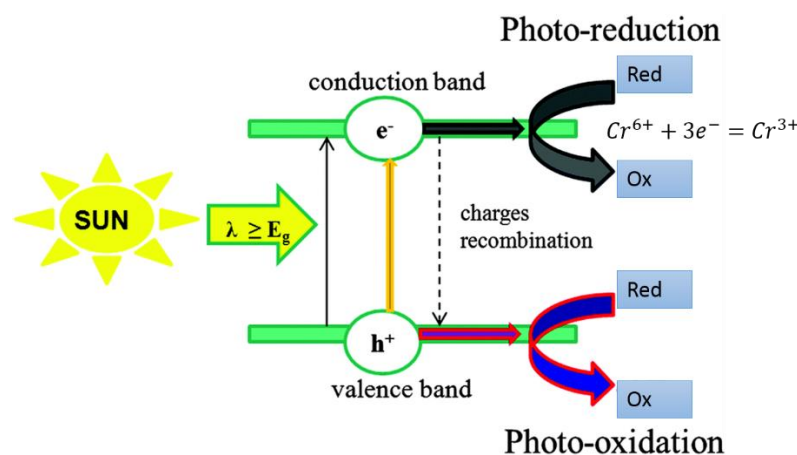


Figure 1.1 Photo-activation of a semiconductor and primary reactions occurring on its surface (Colmenares and Luque, 2014).

### 1.1.3 Photocatalyst materials for reduction of Cr(VI)

A desired photocatalyst must possess high photocatalytic efficiency, high activity, ability to utilize visible and/or near UV light, photostable (durable), reusable, insoluble under most condition, non-toxic, chemically and biologically inert, low density, good biocompatibility and cheap. There are many SC photocatalyst such as NiO (Hashemzadeh et al., 2015), Cu<sub>2</sub>O (Qin et al., 2015), ZnO (Cheng et al., 2015), ZrO<sub>2</sub>

(Rozana et al., 2017),  $\text{Fe}_2\text{O}_3$  (Xu et al., 2012),  $\text{WO}_3$  (Ou et al., 2013) and  $\text{TiO}_2$  (Trejo-Valdez et al., 2019, Rahmat et al., 2018) that can be used for Cr(VI) reduction. Of all different SC photocatalysts reported in literature,  $\text{TiO}_2$  appears to be the most extensively used for photocatalysis processes (Barbeni et al., 1985, Chen and Ray, 1998, Herrmann et al., 1983, Chen and Ray, 2001).

To achieve the photoreduction of Cr(VI), the photogenerated electrons at the CB of the  $\text{TiO}_2$  SC must be more negative than the reduction potential of Cr(VI) ( $\sim -0.36$  eV at pH 7). Since the electrons energy in the conduction band of the SC is  $\sim -0.42$  eV hence the oxide is therefore possible to reduce Cr(VI) to Cr(III). Moreover, the position of CB and VB is influenced by the pH. Higher pH of electrolyte solution will shift the VB and CB towards more cathodic potentials by 59 mV/pH. The reduction potential of Cr(VI) becomes more negative at higher pH than the photogenerated electrons. This leads to the photocatalytic reduction of the Cr(VI) is favoured at a lower pH. Although the driving force of the Cr(VI) reduction decreases with increasing their concentration, it can be reduced photocatalytically to down to  $10^{-12}$  M. According to Chen et al. (2001), since the potential of Cr(III) is more negative than that Cr(VI), it cannot be reduced photocatalytically to lower Cr of lower oxidation states and hence the reduction of Cr(VI) to Cr(III) stops after the Cr(IV) ions have all been transformed to Cr(III). Cr(III) can be precipitated out from the solution by hydroxide treatment.

As mentioned above,  $\text{TiO}_2$  is the most preferred photocatalyst for Cr(VI) removal in environment. Nanostructured  $\text{TiO}_2$  especially in a form of 1-dimensional nanotubes (NTs) and nanowires (NWs) can be fabricated as an effective photocatalyst to reduce Cr(VI) to Cr(III). NTs and NWs have unique and improved properties compared to bulk  $\text{TiO}_2$  due to their high surface area which render them to have higher

surface energy. NTs or NWs with high aspect ratio can facilitate rapid diffusion of free electron to the surface of the photocatalyst for efficient electron transfer process. There are many methods that can be used to produce TiO<sub>2</sub> nanotubes (TNTs) and NWs. In this work, oxidation processes; thermal and anodic were chosen as the methods to produce NWs and NTs respectively.

#### **1.1.4 Anodic and thermal oxidation for TiO<sub>2</sub> Nanotubes and Nanowires Formation**

Many approaches have been employed for the synthesis of TiO<sub>2</sub> with nanotubular structures such as anodic oxidation (Nyein et al., 2016), templating (Kang et al., 2009), sol-gel (Lee et al., 2010), hydrothermal (Suzuki and Yoshikawa, 2004) and photo-electrochemical etching (Macak et al., 2007, Kang et al., 2008). Of these, anodic oxidation is a widely used technique to fabricate TNTs with excellent ordering on a surface of titanium foil (Ghicov and Schmuki, 2009, Macak et al., 2007). Anodization is also preferred because it is a relatively simple (Minagar et al., 2012) and efficient process to fabricate well-aligned TNTs (Gong et al., 2001). Anodization can be conducted in an electrochemical bath with anode (titanium) and cathode (platinum) immersed in fluoride electrolyte. The existence of fluoride ions induces the formation of nanotubes.

On the other hand TiO<sub>2</sub> NW can be synthesized by subjecting titanium foil to high temperature in the presence of oxidising environment with suitable catalyst. The process is a simple, inexpensive and highly scalable process (Arafat et al., 2016).

However, these two methods may induce contamination from the processing route itself. Anodic oxidation for example requires fluoride ions and hence the insertion of the fluoride ions induce the formation of fluoride rich TiO<sub>2</sub> layer which is

not semiconducting. Thermal oxidation as mentioned requires the existence of catalyst like potassium compound, therefore the nanowires formed are often said to comprise of a thin layer of potassium-rich  $\text{TiO}_2$  which can also influence the photocatalytic properties of the oxide. Therefore, despite the success in the formation of the desired nanostructures, the existence of the contamination may influence the properties of the oxide. Hence, in this work, fabrication of compact layer of  $\text{TiO}_2$  using the same anodic and thermal oxidation were done as to compare oxide properties with the nanostructures produced from the process.

## **1.2 Problem Statement**

There are many studies done evaluating the distribution of heavy metal in the coastal and river water in Malaysia. This includes areas in Port Dickson (Praveena and Lin, 2015), Ketam Island in Selangor (Sobihah et al., 2018), Simpang Empat River in Pulau Pinang (Widad and Abdullah, 2013) and Langat River estuary in Selangor (Mokhtar et al., 2015). As mentioned, the toxic Cr(VI) can enter water bodies by unregulated wastewater from electroplating, textile, leather tanning and fertilizer industry. Removal of Cr(VI) can be done by using  $\text{TiO}_2$  as photocatalyst in the photocatalysis process.

However, there are very limited amount of work reported on the use of  $\text{TiO}_2$  for Cr(VI) reduction. Majority of reported works are on the use of  $\text{TiO}_2$  in Advanced Oxidation Process (AOP). AOP is a promising treatment that utilizes highly reactive hydroxyl radicals generated from photogenerated holes for achieving complete mineralization of the organic pollutants such as methylene orange (Taib et al., 2017) into carbon dioxide and water (Krishnan et al., 2017). Reduction on the other hand uses photogenerated electrons in the conduction band of the semiconductor. To date,

there are not many literatures on the use of photoelectrons in TiO<sub>2</sub> to perform reduction of pollutants.

Therefore, in this work, TiO<sub>2</sub> was selected as a photocatalyst semiconductor to reduce Cr(VI), however, to avoid from oxidation of Cr(III) back to Cr(VI), the Cr(VI) solution treated was added with EDTA as scavenger. The EDTA was used to scavenge oxygen (Liu et al., 2017, Tran et al., 2017) and hence oxidation process on TiO<sub>2</sub> will be much reduced. As mentioned, nanostructured TiO<sub>2</sub> such as NWs or NTs is hypothesised to have much better catalytic properties due to the high surface area and high volume ratio it has. There are many reports on the formation of TiO<sub>2</sub> NWs and NTs supported on titanium (Ti) substrate. For the NTs formation, anodic oxidation has been routinely done in fluoride containing electrolyte (Zwilling et al., 1999, Gong et al., 2001, Beranek et al., 2003). The role of the fluoride ions is obvious for the NTs formation. Nevertheless, the NTs contain fluoride contamination in its structure. According to Albu et al. (2008), EDX analysis revealed the presence of fluoride species all over the nanotubular layer which are along the nanotube and at the oxide/metal interface (Habazaki et al., 2007). The TNTs containing fluoride rich layer at the oxide/metal interface can be ascribed to the twice as fast migration rate of the fluoride ions in the high-field barrier oxide (tube bottom). The fluoride has been proved by XPS sputter profiles from the tube bottom sides (Albu et al., 2008). Water soluble (TiF<sub>6</sub>)<sup>2-</sup> (Macak et al., 2008) and TiF<sub>4</sub> complexes are both stable compounds that can be found on the walls of the nanotubes. The fluorine incorporation in the nanotubes is not in the TiO<sub>2</sub> lattice but forming a compound with titanium. This contamination could affect the semiconducting properties of TiO<sub>2</sub>.

On the other hand, one dimensional nanowires fabricated from thermal oxidation of titanium is often done in potassium containing environment. The role of

the potassium ions are obvious for the NWs formation. However, the NWs will have contamination of potassium compound (Lee, 2014). This can be explained by 5-8 % of potassium found in EDX analysis (Cheung et al., 2007). It is assumed that the significant contamination of these elements is due to the process formation itself. Therefore, the performance of those nanostructured TiO<sub>2</sub> as a photocatalyst during the photoreduction of Cr(VI) to Cr(III) may get affected. Nevertheless, there is no work devotes to study on the effect of the contamination from the fabrication process to the properties of the TiO<sub>2</sub>.

Therefore, in this work, thin and compact layer of titanium dioxide was formed by using the same methods to produce the nanotubes and nanowires; anodic and thermal oxidation respectively. The synthesized compact TiO<sub>2</sub> films were expected to be free from any significant contamination as no NH<sub>4</sub>F or KOH was involved in the fabrication process. To the best of knowledge, there is limited amount of publications regarding comparison of photoreduction performance (Cr(VI) to Cr(III)) between TiO<sub>2</sub> nanostructures (NTs and NWs) with compact oxide of TiO<sub>2</sub>, fabricated both by anodic and thermal oxidation.

### **1.3 Research Objectives**

1. To synthesize compact and NTs and NWs of TiO<sub>2</sub> by using anodic and thermal oxidation methods, respectively.
2. To evaluate the Cr(VI) reduction on TiO<sub>2</sub> NTs and NWs by comparing with compact films fabricated by the similar processes.

### **1.4 Research Scope**

This thesis describes the research study on the formation of bulk and nanostructures (NTs and NWs) of TiO<sub>2</sub> by using anodic and thermal oxidation. The



oxidation parameters include presence of  $\text{NH}_4\text{F}$  as etchant, oxidation voltage, presence of  $\text{KOH}$  catalyst and oxidation temperature. The samples were characterized by Field Emission Scanning Electron Microscopy (FESEM), Energy Dispersive X-ray Spectroscopy (EDX), X-ray Diffraction Spectroscopy (XRD), Raman Spectroscopy, Fourier Transform Infrared (FTIR) spectrometer and Transmission Electron Microscopy (TEM). The samples also were used as photocatalyst for  $\text{Cr(VI)}$  removal in simulated  $\text{Cr(VI)}$  solution. The photoactive materials performance were studied via Ultraviolet-Visible (UV-Vis) spectrophotometer.

## **1.5 Thesis Outline**

This thesis consists of five chapters. Chapter 1 explains the background of this research study, problem statements, objectives, research scope and thesis outline. Chapter 2 provides the fundamental knowledge of Ti as a metal,  $\text{TiO}_2$  as a semiconductor material, its properties, crystal structures and importance in applications. The literature review continues with the mechanism of bulk and nanostructures (NTs and NWs) of  $\text{TiO}_2$  formation. In chapter 3, all the materials, chemicals, experimental work procedures and characterization techniques are explained in detail. Chapter 4 contains results and data of the project. The results are analyzed and discussed further. Different microstructures of the compact oxide layer, NTs and NWs of  $\text{TiO}_2$ , phases formation, crystallinity and transformation as well as its photocatalytic performance were presented. Lastly, chapter 5 concludes this research study and give suggestions and recommendation for future work.

## **CHAPTER 2**

### **LITERATURE REVIEW**

#### **2.1 Introduction**

This chapter consists of theories and previous research findings that can be divided into four main parts. Firstly, it is about the main material involved in this project which is  $\text{TiO}_2$ . Its originality, properties, phases and crystal structures are described in details. Secondly, fundamental of nanomaterials,  $\text{TiO}_2$  nanostructures as well as the properties and application are reviewed. The third part reveals two types of synthesis methods which are anodic and thermal oxidation that were used to fabricate the  $\text{TiO}_2$ . Two parameters from each method are elaborated further with the mechanism of each of the material formation. The final part reviews on materials used to reduce Cr(VI) to Cr(III) as well as on the summary of proposed for Cr(VI) reduction by photocatalysts.

#### **2.2 Titanium**

Titanium (Ti) is a very popular metal in metallurgy world which it is known to have an outstanding properties such as high specific strength and excellent corrosion resistant. It was first found by a chemist named William Gregor in 1791. He found it in the form of black sand or also known as ilmenite in Menaccan Valley, Cornwall, England. It is actually titanium iron oxide,  $\text{FeTiO}_3$ . He examined the sand and later named it as manaccanite in regard of the place name. Following that, in Germany, a chemist, Martin Heinrich Klaproth also found a compound containing Ti which is ore rutile,  $\text{TiO}_2$ . Rutile is a common phase of Ti found on the earth. Among all the top titanium producing countries for instance Canada, Norway, China, Japan and United

States of America, Malaysia is also considered as one of the Ti metal producer in the world (Clark et al., 2018, Leyens and Peters, 2003).

There are many ways to classify an element from periodic table. Ti can be categorized as a metallic, non-ferrous transitional, valve and light metal. The separation between light and heavy metal is  $5 \text{ g cm}^{-3}$ . Ti has density of  $4.51 \text{ g cm}^{-3}$ . There are two main crystal structures available for Ti which are hexagonal close-packed (HCP) and body face centered (BCC). Ti has these two crystal structures based on what temperature it experiences. At low temperature, Ti has hexagonal closed packed (HCP) crystal structure or commonly known as  $\alpha$ . Meanwhile, at temperature higher than  $882^\circ\text{C}$ , Ti has body centered cubic (BCC) structure or known as  $\beta$ . The phase transformation from  $\alpha$  to  $\beta$  crystal structure is called as an allotropic transformation. The illustrations of both crystal structures can be seen in Figure 2.1. Table 2.1 depicts comparison between Ti and other metals in terms of their characteristics and properties.

Table 2.1 Characteristics of Ti when compared to other metals (Lütjering and Williams, 2007)

	<b>Ti</b>	<b>Fe</b>	<b>Ni</b>	<b>Al</b>
Melting Temperature ( $^\circ\text{C}$ )	1670	1538	1455	660
Allotropic Transformation ( $^\circ\text{C}$ )	882 ( $\beta$ to $\alpha$ )	912 ( $\gamma$ to $\alpha$ )	-	-
Crystal Structure	BCC HCP	to FCC to BCC	FCC	FCC
Room Temperature E (GPa)	115	215	200	72
Yield Stress Level (MPa)	1000	1000	1000	500
Density ( $\text{g/cm}^3$ )	4.5	7.9	8.9	2.7

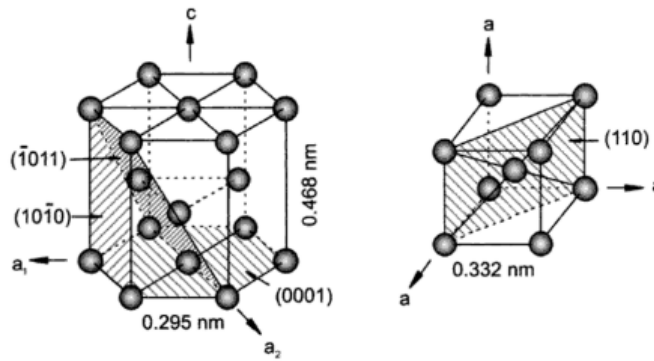


Figure 2.1 Crystal structure of HCP and BCC phase (Layens and Peters, 2003).

In the metallic group, Ti is the fourth most abundant metal found on the earth after aluminium (Al), iron (Fe) and silicon (Si). Meanwhile, Ti is the ninth most abundant element in the earth's crust. Despite the huge amount of the metal, Ti is sold at a very high price. It is heavily used in many fields such as aerospace and biomedical applications.

### 2.3 Titanium dioxide

Titanium dioxide has many importance in many technical field such as in civil as nano-paint (self-cleaning), antibacterial agents, catalysis and photocatalysis. With that, it can be seen that the number of publications on  $\text{TiO}_2$  has been increasing gradually from 1975 and reach a steep gradient at early 2000 (Diebold, 2003). The innovation on  $\text{TiO}_2$  research has been revolutionizing year by year. From bulk structure, to miniaturization and now surface manipulation of the  $\text{TiO}_2$ . This is because of its excellent properties such as low density, excellent biocompatibility and chemical stability. There are quite a number of its application in many technical field for instance (Diebold, 2003),

- As a photocatalyst in heterogeneous catalysis
- To produce hydrogen and electric energy in solar cells

- As a gas sensor to control air/fuel mixture in car engines
- As white pigment in paints and cosmetic products as it has high refractive index
- As a protective coating against environmental damage
- As a self-cleaning coating on car windshields
- As an optical coating in ceramics and in electric devices
- In the biocompatibility of bone implants
- In Li-based batteries and electrochromic devices in nanostructured form

TiO<sub>2</sub> has many different phases. It can be seen in Table 2.2.

Table 2.2 Different phases of TiO<sub>2</sub> (Hanaor and Sorrell, 2011).

<b>Phases of TiO<sub>2</sub></b>
Rutile
Anatase
Brookite
TiO <sub>2</sub> II or srilankite, an orthorhombic polymorphs of the lead oxide structure
Cubic fluorite-type polymorph
Pyrite-type polymorph
Monoclinic baddeleyite-type polymorph

Rutile, anatase and brookite are the only naturally occurring oxide of titanium at atmospheric pressure. Rutile is a stable phase while the other two are metastable. Rutile phase have been investigated extensively. Meanwhile, surface science research on the technologically quite important anatase phase is just starting (Diebold, 2003). And last one is brookite. The last five phases are of high-pressure phases of TiO<sub>2</sub>. They have minor significance for research and development application due to their phase stability issue (Hanaor and Sorrell, 2011). Figure 2.2 shows the crystal structures of anatase, rutile and brookite.

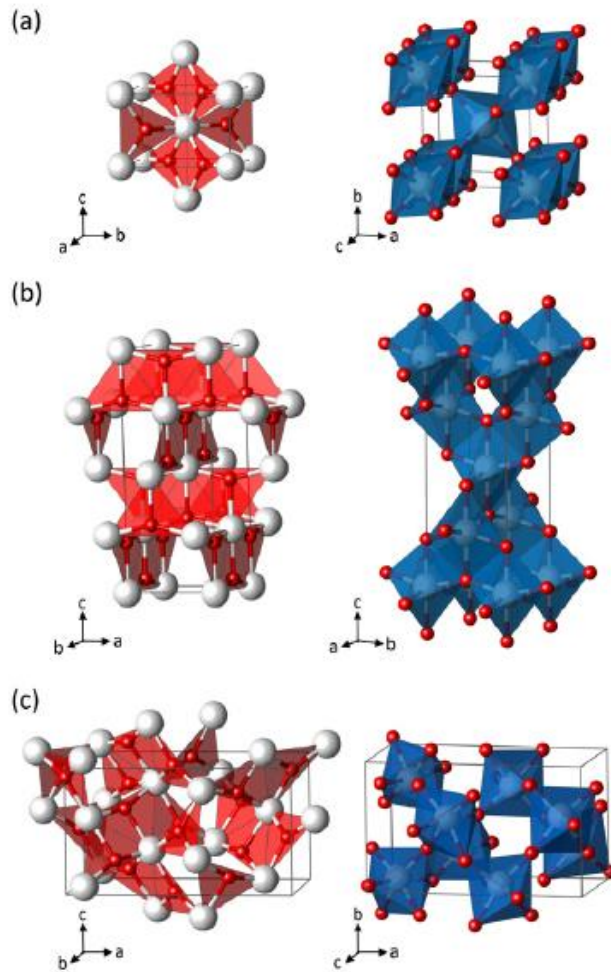


Figure 2.2 Planar  $Ti_3O$  building-block representation (left) and  $Ti_6O$  polyhedral (right) for the  $TiO_2$  phases rutile (a), anatase (b) and brookite (c) (Ti (white); O (red)) (Landmann et al., 2012).

Table 2.3 Bulk properties of titanium dioxide with its crystal structures (Diebold, 2003).

Properties	Crystal structure			Reference
	Anatase	Rutile	Brookite	
<b>Atomic radius (nm)</b>				
<b>O</b>	0.066 (covalent)			
<b>Ti</b>	0.146 (metallic)			
<b>Ionic radius (nm)</b>				
<b>O (-2)</b>	0.14			
<b>Ti (+4)</b>	0.064			
<b>System</b>	Tetragonal	Tetragonal	Rhombohedral	(Diebold, 2003)
	a	0.3733	0.4584	(Diebold, 2003)
	b	-	0.9166	

<b>Lattice constants (nm)</b>	c	0.937	0.2953	0.5135	
	c/a	2.51	0.644	0.944	
<b>Atom per unit cell (Z)</b>		4	2		(Paufler, 1988, Burdett et al., 1987)
<b>Unit cell volume (nm<sup>3</sup>)</b>		0.1363	0.0624		
<b>Density (kg/m<sup>3</sup>)</b>		3830	4240	4170	(Diebold, 2003)
<b>Electrical resistance (<math>\Omega</math> m)</b>	773 K	-	$3 \times 10^5$	-	(Diebold, 2003)
	1073 K	-	$1.2 \times 10^2$	-	
	1473 K	-	$8.5 \times 10^2$	-	
<b>Electron mobility (<math>\mu\text{m}</math>)</b>		$\sim 10$	$\sim 1$	-	(Diebold, 2003)
<b>Calculated indirect bandgap (eV)</b>		3.23-3.59	3.02-3.24		(Beltrán et al., 2006, Madhusudan Reddy et al., 2003, Serpone, 2006)
<b>(nm)</b>		345.4-383.9	382.7-410.1		
<b>Experimental bandgap (eV)</b>		$\sim 3.2$	$\sim 3.0$		(Beltrán et al., 2006, Mardare et al., 2000)
<b>(nm)</b>		$\sim 387$	$\sim 413$		
<b>Refractive index</b>	$n_g$	2.488	2.908	2.7004	(Diebold, 2003)
	$n_m$	-	-	2.5843	
	$n_p$	2.561	2.621	2.5831	
<b>Solubility in water</b>		Insoluble	Insoluble		(Fisher and Egerton, 2001)

### 2.3.1 Rutile

According to many thermodynamics studies, rutile is considered to be more stable than anatase at all temperatures and pressures. In order for anatase to be more stable, negative pressures are needed.

### **2.3.2 Anatase**

As mentioned, TiO<sub>2</sub> can be fabricated by many methods and usually it will first crystallize in anatase form (Okada et al., 2001, Shin et al., 2005). This could be of two reasons. First, structurally, anatase has less-constrained molecular construction compared to rutile. Therefore, it is easier for the short-range ordered TiO<sub>6</sub> octahedra to arrange themselves into a long-range ordered of anatase structure (Matthews, 1976). Secondly, in a thermodynamic angle, it is known that anatase has lower surface free energy compared to rutile. Hence, it can be said that the more rapid recrystallization of anatase is due to that factor although it has higher Gibbs free energy compared to rutile.

### **2.3.3 Semiconductor materials**

Titanium dioxide (TiO<sub>2</sub>) is a semiconductor material that has been studied extensively in the last few decades due to its chemical stability, nontoxicity and high photocatalytic activity (Mahajan et al., 2008). Depending on the crystal phases, TiO<sub>2</sub> has energy band gap ranging from 3.02 eV to 3.59 eV.

## **2.4 Nanostructure of TiO<sub>2</sub>**

### **2.4.1 Nanomaterials**

According to International Organization for Standardization (2015), any material with any external dimension, internal structure or surface structure in the nanoscale is considered as nanomaterial. Following that, nanoscale can be defined as



length range approximately from 1 nm to 100 nm. Nanomaterials can be classified into four main classes: zero, one, two and three dimensional nanomaterials. In this work, one dimensional (1D) of  $\text{TiO}_2$  was fabricated and investigated. Examples of 1D nanomaterials are nanowires, nanorods and nanotubes. These materials have at least one dimension in nanoscale. A bulk material is significantly different than a material in nanoscale (nanomaterial) even though it has the same chemical composition. This is mainly due to the dimensional confinement which leads to having a high surface area to volume ratio. For example, bulk Pt is an inert material. It remains unaffected with any single mineral acid. However, in nanoscale, Pt is very reactive that it can act as a catalyst in a catalytic activity (Bai et al., 2016). The higher surface area to volume ratio of a material, the higher reactive it gets towards its environment. Similarly,  $\text{TiO}_2$  in nanoscale can have properties which are markedly different than bulk material.

Nanomaterial fabrication can be divided into two categories which are bottom up and top down approach. Bottom up approach can be defined as building up of any dimensional category of nanomaterial from the bottom. It can be atom by atom, molecule by molecule or cluster by cluster. For example, sol-gel, templated, and salt reduction. Meanwhile, top down approach can be defined by slicing or successive cutting of a bulk material to get nano-sized particles. For instance, milling, etching and lithography methods. As mentioned, anodic and thermal oxidation methods were used in this work.

#### **2.4.2 Nanostructure of $\text{TiO}_2$**

A good photocatalyst must have a high surface area for more catalytic sites. Nanoparticles are zero dimensional nanomaterials which have a higher surface area compared to NTs and NWs which are 1D nanomaterials. However, many literatures

stated that 1D TiO<sub>2</sub> has better photocatalytic reaction compared to nanoparticles. Figure 2.3 shows comparison of electron pathways through nanoparticles NTs and NWs. Although TiO<sub>2</sub> NPs have higher surface area compared to NTs and NWs, they have shorter diffusion length of the electron, hence increasing recombination of the electrons (Javed et al., 2014). Moreover, 1D geometrical structure of TNTs facilitates rapid diffusion-free electron transport along the longest direction and reduce interface charge recombination greatly. Nevertheless, the characteristic of a material is always associated with the fabrication processes. The challenge remains which is to investigate the exact properties of the 1D TiO<sub>2</sub> derived by processes which allows for perfect its formation and to compare with bulk material.

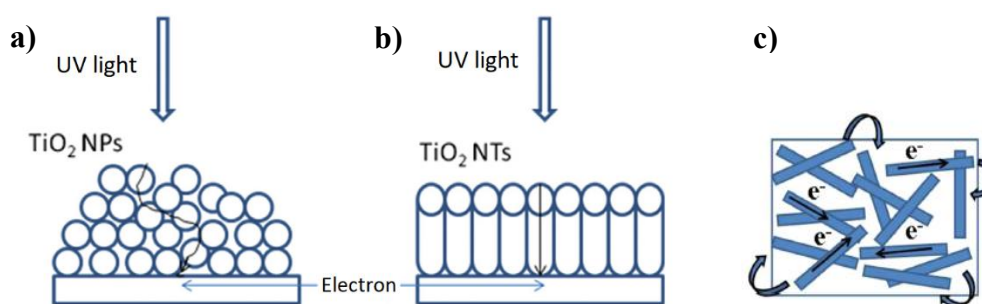


Figure 2.3 Comparison of electron pathways through TiO<sub>2</sub> nanoparticles (NPs), nanotubes (NTs) and nanorods (NRs). (a-b) (Javed et al., 2014) (c) (Sengupta et al., 2016)

## 2.5 Synthesis of titanium dioxide

There are many fabrication techniques that can be used to produce TiO<sub>2</sub> in the form of 1D nanotubes or nanowires depending on what is desired for the end application. As for photocatalyst, supported oxide NTs on a metal substrate is preferred as it will be easier to remove the catalyst after use. Several methods have been identified to grow oxide on metal substrate. One relatively straight forward process is by oxidizing the metal substrate either by polarizing it in an electrochemical bath or by heating it up at

high temperature in an oxidizing environment. Both processes will result in the formation of thin oxide film of the parent metal. Oxidising titanium results in the formation of TiO<sub>2</sub> film.

### **2.5.1 Electrochemical anodic oxidation method**

Anodization is an electrochemical process conducted on a metal to produce a layer of metal oxide on the metals surface. The anodization process is performed in an electrochemical cell consisting of two electrodes, the working electrode or the anode and the counter electrode or the cathode. The metal is employed as an anode and oxidation process starts on the anode when external voltage is applied between anode and cathode electrodes in an electrolyte (Abedinisohi, 2013). Electrochemical anodic oxidation or so called anodization is a well-established method to produce metal oxide (Sibert, 1963). This method has been used to grow a thick and uniform oxide layer on metals for a decade or so (Minagar et al., 2012). Anodic oxidation is a widely used technique to fabricate TiO<sub>2</sub> film comprising of self-ordered nanotubular structure, because it is a relatively simple and efficient process to fabricate well-aligned and highly ordered NTs. Figure 2.4 is a schematic drawing of an electrochemical anodization cell. Often, Pt is used as the cathode while Ti is used as the anode. Moreover, anodization can produce TiO<sub>2</sub> nanotube layer which grows normal to the surface with regular diameter, in contrast with other techniques such as solvothermal and hydrothermal methods, in which nanotubes are obtained in a free form but have a lower degree of organization (Dumitriu et al., 2015, Ng et al., 2010).

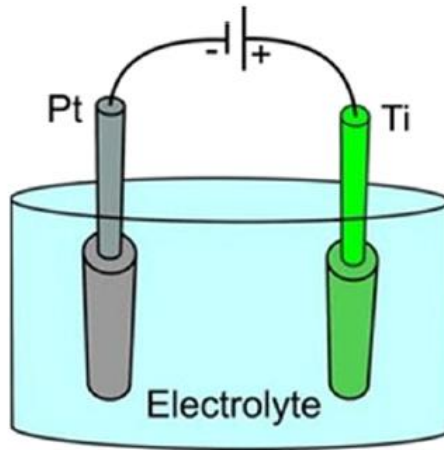


Figure 2.4 Schematic drawing for Titanium anodization cell (Galstyan et al., 2013).

### 2.5.1(a) Mechanism of compact and dense TiO<sub>2</sub> formation

The formation of oxide by electrochemical process is a well-documented topic. At the beginning of the anodization where the voltage is applied, polarization happens at the Ti metal foil surface (Equation 2.1). Then in the presence of oxidants, oxide will form (Equation 2.2 – 2.3). Anodic oxidation can be represented by Equation 2.4 (Brunette et al., 2012).



When the anodic electrolyte is comprised of only oxidant, the resulting film is often compact. TiO<sub>2</sub> has low conductivity compared with the electrolyte and the metal substrate, therefore the ions and charge transfer from the electrolyte to the metal surface, and vice versa, are controlled by the applied voltage.

With the absence of fluoride ions in the electrolyte, a layer of metal oxide will be formed according to the Equation 2.3 and 2.4, where the oxygen ions required for the oxidation process are supplied by water molecules within the electrolyte. As the oxide layer has a low conductivity, it works as an insulator, which hinders the transport of oxygen and titanium ions, the continued growth of the oxide layer has controlled by field aid. As there is no fluoride source in the electrolyte, no chemical dissolution occur for further pore growth. Figure 2.5 is a schematic drawing for the anodization of titanium in an electrolyte free from fluoride (Taveira et al., 2005).

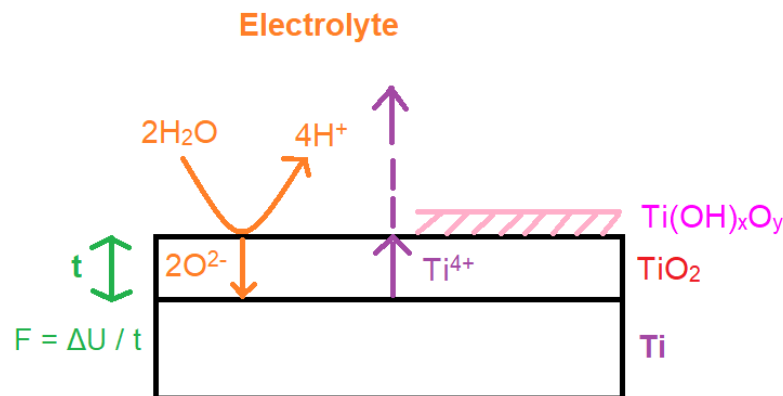


Figure 2.5 Schematic drawing for anodization of titanium in an electrolyte free from fluoride ions (Macak et al., 2007)

### 2.5.1(b) Mechanism of nanotubes TiO<sub>2</sub> formation

Nevertheless, when fluoride ions are added in the electrolyte, the oxide formation is accompanied by chemical dissolution processes. In fluoride electrolyte, three consecutive steps for nanotubes formation are (Awad et al., 2017, Keller et al., 1953, Khudhair et al., 2016):

- Initial stage: polarisation of Ti, where dissolution of Ti and the formation of the Ti ions that dissolve in the solution can happen
- Intermediate stage: the interaction of Ti<sup>4+</sup> with oxygen ions supplied by the water molecules in the electrolyte to form TiO<sub>2</sub> on titanium surface

- Steady state: chemical dissolution of the oxide forming porous TiO<sub>2</sub> which then followed by steady state competition between oxide formation and oxide dissolution reactions for nanotubes formation

The oxide grows as a result of the movement of ions under the action of an applied electric field. As the oxide film grows thicker and its overall electrical resistance increases, it acts as a barrier to the flow of ions and electrons. The oxide that is formed is generally a barrier type film. The anodizing ratio, defined as the maximum oxide thickness obtainable per unit volt, is in the range 1–3 nm/V. The presence of a pore free barrier layer limits the final thickness of the oxide to within a few hundred nanometers.

TNTs can be formed by using certain kinds of electrolytes. Self-organized TiO<sub>2</sub> layers can be formed using fluoride containing electrolyte. Meanwhile, bundles of TNTs (i.e. not self-organized) can be formed by using perchlorate, chloride, bromide or sulphuric acid containing electrolytes.

This typical current density (mA/cm<sup>2</sup>) against time (s) graph as in Figure 2.6 can be obtained during anodization process. It can be seen that there are three significant stages in the process. The first stage, from a – b, polarization occur due to coulombic attraction between positive charge and negative charge. The positive charge comes from the metal which is Ti<sup>4+</sup>. Meanwhile, negative charge comes from the electrolyte which are O<sup>2-</sup> and OH<sup>-</sup>. In addition, F<sup>-</sup> also involve for fluoride-containing electrolyte. After that, an oxide barrier layer of TiO<sub>2</sub> starts to form. Therefore, it can be seen in the first stage, current decreases. Oxidation process continue to occur forming a very high resistance oxide barrier layer (Regonini et al., 2013).